Springer

KSME

Journal of Mechanical Science and Technology 26 (3) (2012) 653~659
www.springerlink.com/content/1738-494x
DOI 10.1007/s12206-011-1201-6

Vibration analysis on the rolling element bearing-rotor system of an air blower †

Wu Hao[1,2], Zhou Qiong[1], Zhang Zhiming[1] and An Qi[1,*]

[1]*School of Mechanical and Power Engineering, East China University of Science and Technology, Shanghai 200237, China*
[2]*Shanghai Institute of Special Equipment Inspection and Technology Research, Shanghai, 200333, China*

(Manuscript received October 8, 2010; Revised August 13, 2011; Accepted October 25, 2011)

Abstract

Air blowers are widely used in industry. The vibration of the rolling bearing-rotor is a key factor in the blower's performance because it significantly influences the security and working life of the whole system. In previous research on the vibration characteristics of the air blower, the supporting rolling element bearing was always simplified as a particle on a shaft with radial stiffness and damping coefficient. Such simplification neglects the effects of the bearing structure on the vibration performance of the rotor system. In this paper, a numerical model of the bending stiffness of the tapered roller bearing was established through mechanics and deformation analysis. On the base of the model, a new TMM (transfer matrix method) for bearing-rotor system was established; the new TMM considers the influences of the bearing structure on the vibration of the rotor system. Furthermore, modal analysis on an air blower rotor system was carried out by using the new TMM, and the mode shape, critical speed and unbalance response of the air blower system were obtained. The same blower rotor was also analyzed by FEM to verify the validation of the new TMM, showing that the new method proposed in this paper for vibration characteristics calculation of an air blower is credible.

Keywords: Air blower; Bearing-rotor system; Transfer matrix method; Vibration

1. Introduction

Air blowers, with rotors supported by rolling element bearing, are widely used in industry. In application, air blowers often face many different problems which will influence the working process of a factory. One of the most common problems of air blowers is vibration. The vibration calculation of air blowers is a focus in the power engineering field. The blower's vibration mainly originates from the oscillations of the blower's shell and bearing-rotor system [1-3], with the bearing-rotor system as the primary source. The most important vibration parameters of the air blower rotor include critical speed, unbalanced response, etc. To obtain these parameters, the stiffness and damping of the supporting rolling element bearing should first be calculated, and then the governing equations of the whole system can be established. On these bases, the dynamic characteristics of the air blower rotor system can be revealed and the vibration parameters can be obtained.

Previous researchers who focused on the vibration of radial ball bearings were Rahnejat and Gohar [4]. They built a deep groove ball bearing model including an extrapolated equation with effect of squeeze-film. They suggested that the limit cycle frequency and amplitude of the ball bearing is affected by the number of balls, applied load and radial internal clearance. Even in the presence of elastohydrodynamic lubricating film between balls and the raceways, a peak of the ball passage frequency (BPF) appears in the spectrum. Aini et al. [5, 6] used five-degree-of-freedom model of rolling element bearing and represented the bearings by nonlinear springs considering elastohydrodynamics effects. Rahman et al. [7] extended Aini's work by investigating the free vibration response of a horizontally mounted multi-bearing spindle system. They analyzed different bearing settings of the front bearing sets and variation in axial preload. Then they [8] showed BPF and its harmonics due to non-linear Hertzian contact between the balls and the raceways for a defect free bearing. Karacay et al. [9] proposed a vibration model of a ball bearing with waviness considering three degrees of freedom.

Wu et al. [10, 11] obtained the exact solution of a single-span non-uniform Timoshenko beam carrying number of spring-mass systems by using lumped-mass and continuous-mass transfer matrix method, respectively. Yong et al. [12] presented transfer matrix solutions to study the axisymmetric and non-axisymmetric consolidation of a multilayered soil system under arbitrary loading.

Liew et al. [13] studied transient response on deep groove ball bearing-asymmetric elastic rotor by transfer matrix me-

† This paper was recommended for publication in revised form by Associate Editor Ohseop Song

* Corresponding author. Tel.: +86 21 64251834, Fax.: +86 21 64251834
E-mail address: anqi@ecust.edu.cn

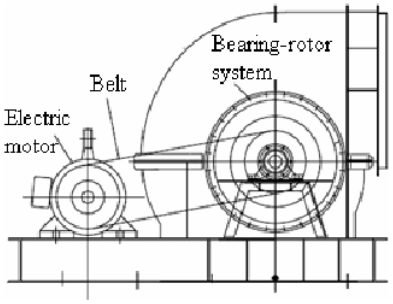

Fig. 1. Configuration of the air blower.

thod. He obtained load distribution on each roller element and solved kinematic equations for the bearing-rotor system by Range-Kutta method. Rui et al. [14] developed a discrete time transfer matrix method of a multi-body system to study general multi-body system dynamics by combining and expanding the transfer matrix method and the numerical integration procedure. Hsieh et al. [15, 16] developed a modified transfer matrix method for analyzing the coupled lateral and torsion vibrations of the symmetric/asymmetric rotor-bearing system with an external perturbing torque.

From the above literatures, it can be seen that in the past research about the vibration characteristics of a bearing-rotor system, the bearing was separated from the system and was treated as a point with stiffness and damping, which neglects the influences of bearing structure on the bearing-rotor system. In fact, the rolling element bearing structure influences the stiffness of the shaft significantly.

In this paper, the analytical model for calculating overall radial stiffness and overall damping of the tapered roller bearing, and the numerical model for calculating bending stiffness of the tapered roller bearing are established. On such basis, new TMM and vibration equations of the bearing-rotor system taking into consideration rolling element bearing structures were established. An actual air blower was analyzed with the new TMM to show that the bearing structure significantly affects the vibration characteristics of a bearing-rotor system. The rotor was also analyzed by FEM and results were verified, which shows that the new method proposed for vibration characteristics calculation of air blowers in this paper is credible.

2. A new transfer matrix method

2.1 Deformation analysis of bearing-rotor system

Fig. 1 shows an air blower used in a power station in China. It is mainly composed of a motor, pulley and bearing-rotor. The most important part of the blower is its rolling bearing-rotor system. During the vibration analysis of bearing-rotor system, the foundation is treated as rigid and its vibration is ignored.

Fig. 2 shows the geometry parameters of the rolling bearing-rotor system, which is composed of an impeller, pulley, shaft and a pair of tapered roller bearings (30218). The impeller, located in the middle of the two bearings, is composed of

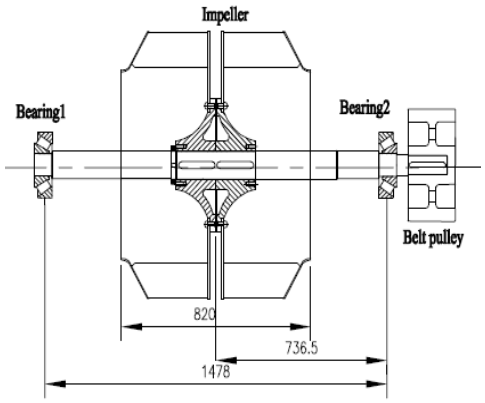

Fig. 2. Configuration of bearing-rotor system of the air blower.

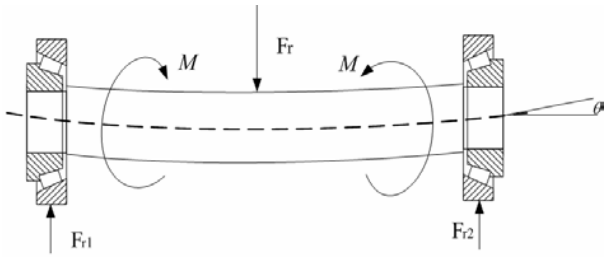

Fig. 3. Bending deformation of the tapered roller bearing-rotor system.

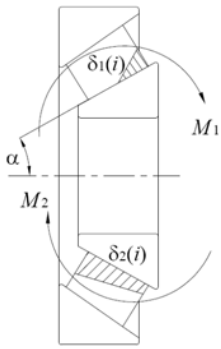

Fig. 4. Deformation of the tapered roller bearing under bending moment.

several bar pieces of weight 264.45 kg and inertia 37.49 $kg \bullet m^2$; the pulley located on the right side of the shaft has a weight of 158.97 kg with inertia 3.27 $kg \bullet m^2$ and the rotor's working speed is 6000 rpm. According to lumped mass method, the beam is simplified to be several disks and beams, and the disk is considered to have no thickness and the beam is considered to have no mass.

As Fig. 3 shows, the air blower rotor is supported by two tapered roller bearings. Under the action of radial load, the shaft bends, and bending moments by an external radial load will act upon the two bearings. Under the radial load, the shaft will produce radial elastic displacement and produce a tilting angle between the inner and outer raceways of bearings.

As Fig. 4 shows, for the tapered rolling bearing, the contact

angle is α , conical angle is 2β and the angle between neighbor roller center lines is ψ . Under combined actions of radial load and bending moment, the bearing will deform.

Each rolling element is divided into *n* sections uniformly along the generatrix, and then they are analyzed separately according to the upper and lower half circle.

$$\delta_1(i)=\theta\left(\frac{L}{2}-i\frac{L}{n}\right) \tag{1}$$

where $x\in\left[0,\frac{L}{2}\right]$, $q=0$ when $\delta\le 0$.

For the bottom roller, the deformation on the i th section is

$$\delta_2(i)=\delta_{\mathrm{r}}+i\theta\frac{L}{n},\quad x\in[0,L]. \tag{2}$$

For the rollers in upper circle, the deformation on the i th section is

$$\delta_{1j}(i)=\delta_1(i)\cos j\psi . \tag{3}$$

For the rollers in the lower circle, the deformation on the i th section is

$$\delta_{2j}(i)=\delta_2(i)\cos j\psi . \tag{4}$$

According to Hertz contact theory [17], stress distribution along the roller generatrix under radial force and bending moment can be expressed as:

$$\begin{cases}\delta_{1j}(x)=A\bullet q_{1j}(x)+B\bullet q_{1j}(x)\ln q_{1j}(x)\\ \delta_{2j}(x)=A\bullet q_{2j}(x)+B\bullet q_{2j}(x)\ln q_{2j}(x)\end{cases}. \tag{5}$$

2.2 Mechanics analysis of bearing-rotor system

The bending moment acting on the tapered rolling bearing can be obtained as

$$M=M_1+M_2 \tag{6}$$

where

$$M_1=\sum_{j=1}^{Z}\sum_{i=1}^{n}\left(L-\frac{i}{n}L+D_0\sin\alpha\right)q_{1j}(i)$$
$$M_2=\sum_{j=1}^{Z}\sum_{i=1}^{n}\left(L-\frac{i}{n}L+D_0\sin\alpha\right)q_{2j}(i)$$

where $q_{1j}(i)$ and $q_{2j}(i)$ can be obtained by Eq. (5). Because there is an implicit function in Eq. (5), bending moment of bearing should be solved using Newton-Raphson iterative method for Eqs. (5) and (6). When the tolerance between adjacent calculation results of M is 2×10^{-4}, the result can be considered reliable.

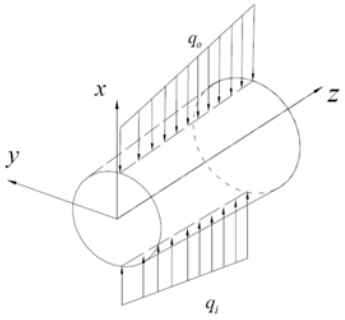

(a) Load distribution on single roller

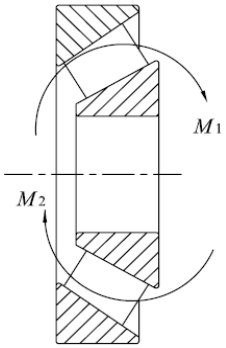

(b) Load distribution on bearing

Fig. 5. Load distribution on roller and bearing.

By the above equations, the bending moment and tilting angle can be obtained. According to the definition of stiffness, the bending stiffness of the tapered roller bearing can be obtained as:

$$k_{\mathrm{r}}=\frac{dM}{d\theta} . \tag{7}$$

Fig. 5 shows the stress distribution and the moment on single rolling element and the whole bearing.

2.3 Radial stiffness and damping of the tapered roller bearing

According to the authors' past research [18, 19], radial stiffness of tapered roller bearing is

$$\begin{aligned}K_c&=\lim_{\substack{\Delta F_r\to0\\ \Delta\delta\to0}}\frac{\Delta F_r}{\Delta\delta}\\ &=\lim_{\Delta F_r\to0}\frac{1}{n+mF_r\dfrac{\ln(F_r+\Delta F_r)-\ln F_r}{\Delta F_r}+m\ln(F_r+\Delta F_r)+C\left[\dfrac{F_r^{-0.13}-(F_r+\Delta F_r)^{-0.13}}{\Delta F_r}\right]}\\ &=\frac{1}{n+m+m\ln F_r+0.13C\cdot F_r^{-1.13}}\end{aligned} \tag{8}$$

and radial damping of tapered roller bearing is

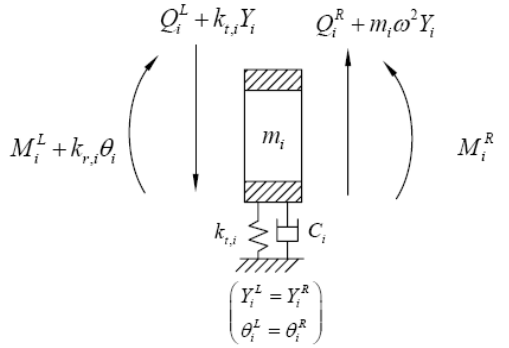

Fig. 6. New station of bearing.

$$C'=\frac{1}{\frac{1}{C_1}+\frac{1}{C_2}}. \tag{9}$$

2.4 New transfer matrix method

There is a tilt angle between inner and outer raceways besides radial compression; the tilt angle changes state vectors transfer relation of roller bearing, as Fig. 6 shows.

Bearing station transfer relation considering bearing geometry structure is

$$\begin{cases} Y_i^R = Y_i^L = Y_i \\ \theta_i^R = \theta_i^L = \theta_i \\ M_i^R = M_i^L + k_{r,i}\theta_i^L \\ Q_i^R = Q_i^L + \left(k_{t,i} + i\omega C_i - m_i\omega^2\right)Y_i^L \end{cases} \tag{10}$$

where Y_i^L, θ_i^L, M_i^L and V_i^L denote the transverse displacement, slope, bending moment and shearing force at left side of station i respectively, while Y_i^R, θ_i^R, M_i^R and V_i^R denote the same quantities at the right side of station i respectively. k_t and k_r denote the bearing radial and bending stiffness respectively, ω denotes the rotating speed of the shaft and C denotes the radial damping of the roller bearing.

Writing Eq. (10) in a matrix form gives

$$\begin{bmatrix} Y \\ \theta \\ M \\ Q \end{bmatrix}_i^R = [T_S]_i \begin{bmatrix} Y \\ \theta \\ M \\ Q \end{bmatrix}_i^L \tag{11}$$

where $[T_S]_i$ is the transfer matrix of station i,

$$[T_S]_i = \begin{bmatrix} 1 & 0 & 0 & 0 \\ 0 & 1 & 0 & 0 \\ 0 & k_{r,i} - J_i\omega^2 & 1 & 0 \\ k_{t,i} + i\omega C_i - m_i\omega^2 & 0 & 0 & 1 \end{bmatrix}.$$

Setting K_t and C as 0 generates station transfer matrix $[T_Q]_i$

$$[T_Q]_i = \begin{bmatrix} 1 & 0 & 0 & 0 \\ 0 & 1 & 0 & 0 \\ 0 & -J_i\omega^2 & 1 & 0 \\ -m_i\omega^2 & 0 & 0 & 1 \end{bmatrix}. \tag{12}$$

By Eqs. (11)-(13) the overall transfer matrix of the system can be obtained:

$$\begin{bmatrix} Y \\ \theta \\ M \\ Q \end{bmatrix}_{i+1}^L = [T]_i \begin{bmatrix} Y \\ \theta \\ M \\ Q \end{bmatrix}_i^L \tag{13}$$

where $[T]_i$ denotes the transfer matrix of section i

$$[T]_i = [T_Q]_i [T_s]_i.$$

From Eq. (13) it can be seen that the state variables at the left side of station $i+1$ may be obtained from those at the left side of station i.

Replacing $\begin{bmatrix} Y \\ \theta \\ M \\ Q \end{bmatrix}$ by $\{\delta\}$ and repeating application of transfer Eq. (13) yields the following relationships:

$$\{\delta\}_2^L = [T]_1\{\delta\}_1^L$$
$$\{\delta\}_3^L = [T]_2\{\delta\}_2^L = [T]_2[T]_1\{\delta\}_1^L$$
$$\{\delta\}_4^L = [T]_3\{\delta\}_3^L = [T]_3[T]_2[T]_1\{\delta\}_1^L$$
$$\cdots\cdots$$
$$\{\delta\}_{n+1}^R = [T]_n\{\delta\}_n^L = [T]_n\cdots[T]_3[T]_2[T]_1\{\delta\}_1^L$$
$$\{\delta\}_{n+1}^R = [T_s]_{n+1}\{\delta\}_{n+1}^L = [T_s]_{n+1}[T]_n\cdots[T]_3[T]_2[T]_1\{\delta\}_1^L = [\bar{T}]\{\delta\}_1^L$$

where $[T_s]_{n+1}$ denotes transfer matrix of station $n+1$; $[\bar{T}]$ denotes the overall transfer matrix of the rotor system.

$$[\bar{T}] = [T_s]_{n+1}[T]_n\cdots[T]_3[T]_2[T]_1 = \begin{bmatrix} T_{11} & T_{12} & T_{13} & T_{14} \\ T_{21} & T_{22} & T_{23} & T_{24} \\ T_{31} & T_{32} & T_{33} & T_{34} \\ T_{41} & T_{42} & T_{43} & T_{44} \end{bmatrix} \tag{14}$$

By the overall transfer matrix, the relationship between the state variables at the left side of the beam $\{\delta\}_1^L$ and those at the right side of the beam $\{\delta\}_{n+1}^R$ can be obtained. Substituting

Fig. 7. Transfer matrix model of bearing-rotor system.

boundary conditions $M_1^L = 0, Q_1^L = 0$
$M_{n+1}^R = 0, Q_{n+1}^R = 0$ into Eq. (13), leads to

$$\begin{cases} T_{31}Y_1^L + T_{32}\theta_1^L = 0 \\ T_{41}Y_1^L + T_{42}\theta_1^L = 0 \end{cases} . \tag{15}$$

Non-trivial solution for Eq. (15) requires that

$$\Delta(\omega) = \begin{vmatrix} T_{31} & T_{32} \\ T_{41} & T_{42} \end{vmatrix} = 0 \tag{16}$$

.

Eq. (16) is the frequency equation of a beam and can be used for determining the critical speed of the beam. Corresponding to each natural frequency ω_j, there will be a corresponding mode shape. If the boundary conditions are given by $M_1^L = Q_1^L = 0$ and the initial state variables are given by $\begin{Bmatrix} Y_1^L \\ \theta_1^L \\ M_1^L \\ Q_1^L \end{Bmatrix} = \begin{Bmatrix} 1 \\ -T_{31}/T_{32} \\ 0 \\ 0 \end{Bmatrix}$, then the ratio of displacement and the slope on any point of shaft can be obtained.

3. Modal analysis on the air blower

3.1 Calculating results of new TMM

According to the lumped mass method, bearing-rotor system of the air blower is simplified as a combination of no thickness disks and massless beams, and the bearing is simplified as the combination of radial stiffness, damping and bending stiffness coefficients. Fig. 7 shows the lumped mass model.

According to numerical calculating model, the bending stiffness of the tapered roller bearing is $6.38\times10^4\,\mathrm{N\cdot m/rad}$. Substituting the bending stiffness value and lumped mass model of the air blower into the new TMM, the vibration characteristics can be calculated. Fig. 8 shows the first two modal shapes of the air blower. According to TMM, the first critical speed is 2167 rpm, and the second critical speed is 4819 rpm.

Fig. 9 shows the unbalance response amplitude of the center of air blower's impeller. It can be seen that at the rotating speed of 945 rpm, the first unbalanced response amplitude at the center of the air blower is $0.96\times10^{-4}\,\mathrm{m}$, and at the rotating speed of 1790 rpm, the second unbalance response amplitude is $1.17\times10^{-4}\,\mathrm{m}$.

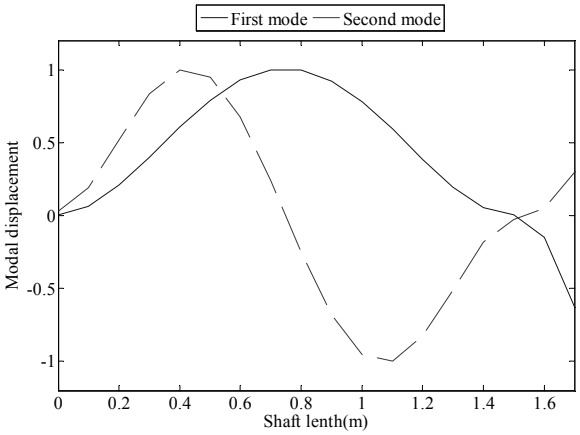

Fig. 8. Mode shape accomplished by TMM.

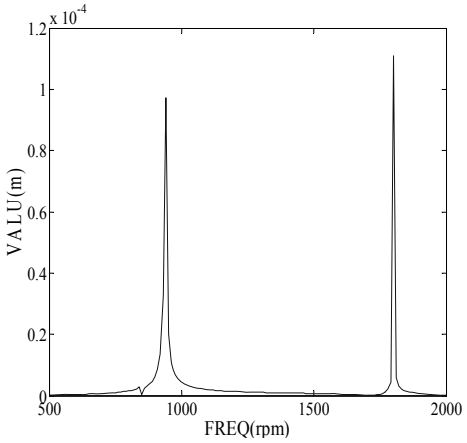

Fig. 9. Unbalanced response calculated by the new TMM.

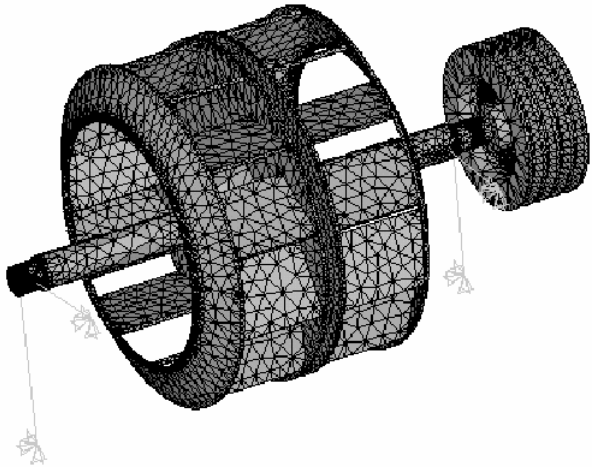

Fig. 10. Finite element model of the bearing-rotor system.

3.2 Calculating results by FEM

Ansys11.0 is used for modal analysis to the same air blower rotor. Fig. 10 shows the FEM model of the air blower rotor.

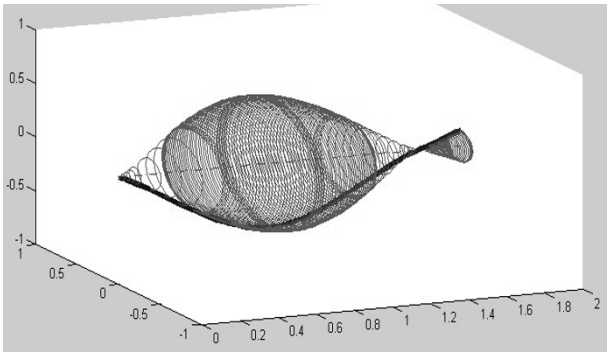

(a) First mode shape calculated by FEM

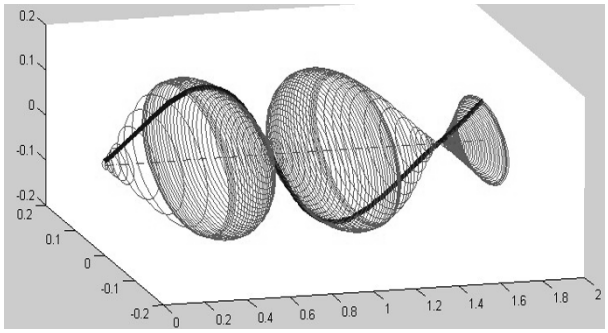

(b) Second mode shape calculated by FEM

Fig. 11. Mode shape accomplished by FEM.

Solid 45 is used, which has 8 nodes and 6 freedoms. Combine14 is used to simulate the tapered roller bearing and axial freedom of the system is limited. Since the geometry is complex, the element shape in mesh process we used is Quad. Standard method has been chosen to solve the problem. In this finite element analysis, tapered roller bearings are simulated by Combine14, and axial freedom of the system is limited.

The governing equations of the whole FEM model is

$$[M]\{\ddot{x}\}+[K]\{\dot{x}\}+[C]\{x\}=\{F\} \tag{17}$$

where $[M]$ denotes mass matrix, $[K]$ denotes stiffness matrix, $[C]$ denotes damping matrix.

The governing equations of each node is

$$\{u\}=\{\varphi\}_i\cos(\omega_i t) \tag{18}$$

where $\{\varphi\}_i$ denotes the *i*th modal vectors, ω_i denotes the *i*th natural frequency. Submitting Eq. (18) into (17), the natural frequency can be obtained. Through modal expansion, each modal shape curve can be obtained.

Fig. 11 shows the first two modal shapes of the air blower rotor. It can be seen that modal shapes obtained by FEM are quite similar to TMM. Both of them reflect the influences of the bearing structure on the rolling element bearing-rotor system.

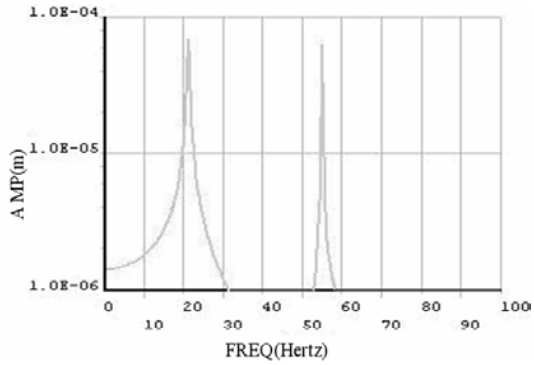

Fig. 12. Unbalanced response calculated by FEM.

Fig. 12 shows unbalance response curves of the air blower rotor. It can be seen that the first unbalance response amplitude is 0.9×10^{-4} m , the second response amplitude is almost the same. According to FEM, the first critical speed is 2005 rpm, and the second critical speed is 4363 rpm.

4. Conclusions

(1) The vibration characteristics of an air blower rotor supported by tapered roller bearings is studied. Through mechanics analysis, the numerical calculating model for structure stiffness of the tapered roller bearing is established and introduced into the vibration analysis for rolling element bearing-rotor system. Considering structure stiffness, radial stiffness and damping of the bearing, a new state vectors relationships between two ends of bearing is established. On this basis, a new TMM is established.

(2) Modal analysis on an air blower is carried out by simultaneous use of the new TMM and FEM. The first critical speed according to TMM(2167) is 8.8% faster than that according to FEM(2005), and the first unbalanced response amplitude at the center of air blower according to TMM(0.96×10^{-4} m) is 6.7% greater than that according to FEM(0.9×10^{-4} m). Furthermore, Fig. 8 (TMM) and Fig. 11 (FEM) show similar mode shapes considering bearing structures. The comparisons show that the new TMM in this paper is credible.

Acknowledgment

This work was supported by ECSUT (East China University of Science and Technology) and SSEI (Shanghai Institute of Special Equipment Inspection and Technology Research).

Nomenclature

E	: Young modulus, *MPa*
ν	: Poisson's ratio
F_r	: Radial force, *N*
l	: Roller length, *m*
n_i	: Rotating speed, *rpm*
p	: Lubricate film pressure, *Pa*

q : Load unit length along roller generatrix, N/m
A_1, A_2, A_3, m, n are middle coefficients,

where

$$A_1 = \frac{1}{2}\frac{1+\tan\beta\tan 2\beta}{\cos\beta+\sin\beta\cdot\tan 2\beta}$$

$$A_2 = \frac{1}{2}\frac{1+\tan\alpha\tan 2\alpha}{\cos\alpha+\sin\alpha\cdot\tan 2\alpha}\frac{\sin\alpha}{\sin\beta},$$

$$A_3 = \frac{1}{2}\frac{1+\tan(\alpha+2\beta)\tan 2(\alpha+2\beta)}{\cos(\alpha+2\beta)+\sin(\alpha+2\beta)\cdot\tan 2(\alpha+2\beta)}\frac{\sin(\alpha+2\beta)}{\sin\beta}$$

$$m = -\frac{2.60\cos(\alpha+\beta)}{ZlE'\cos\alpha} - \frac{8.16\cos(\alpha+\beta)}{ZlE'\cos(\alpha+2\beta)}$$

$$n = \frac{2.60\cos(\alpha+\beta)}{ZlE'\cos\alpha}\left[\ln\frac{D_1ZlE'(A_1+A_2)\cos\alpha}{2}+0.58\right]$$

$$-\frac{8.16\cos(\alpha+\beta)}{ZlE'\cos(\alpha+2\beta)}\left[\frac{1}{2}\ln\frac{D_1A_1A_3}{2ZlE'(A_3-A_1)\cos(\alpha+\beta)}+0.51\right].$$

References

[1] Y. Ohta and E. Outa, Evaluation and prediction of blade-passing frequency noise generated by a centrifugal blower, *ASME Journal of Turbo machinery*, 118 (3) (1996) 597-605.

[2] H. Sun and S. Lee, Numerical prediction of centrifugal compressor noise, *Journal of Sound and Vibration*, 269 (1) (2004) 421-430.

[3] M. Younsi and F. Bakir, Numerical and experimental study of unsteady flow in a centrifugal fan, *Proc. IMechE : Journal of Power and Energy*, 221 (7) (2007) 1025-1036.

[4] H. Rahnejat and R. Gohar, The vibrations of radial ball bearings, *Pro. of the Institution of Mechanical Engineers-Part C-Mechanical engineering science*, 199 (C3) (1985) 181-193.

[5] R. Aini and H. Rahaejat, A five degrees of freedom analysis of vibrations in precision spindles, *International Journal of Machine Tools and Manufacture*, 30 (1) (1990) 1-18.

[6] R. Aini and H. Rahnejat, Vibration modeling of rotating spindles supported by lubricated bearings, *Journal of Tribology*, 124 (1) (2004) 158-165.

[7] A. K. Rahman and R. Aini, On the performance of multi-support spindle-bearing assemblies, *Proc. of Institution of Mechanical Engineers-Part K-Journal of Multi-body Dynamics*, 216 (2) (2002) 117-132.

[8] N. Akturk and M. Uneeb, The effects of number of balls and preload on vibrations associated with ball bearings, *Journal of Tribology*, 119 (1997) 747-753.

[9] T. Karacay and N. Akturk, Vibrations of a grinding spindle supported by angular contact ball bearings, *Proc. of Institution of Mechanical Engineers-Part K-Journal of Multi-body Dynamics,* 222 (2008) 61-74.

[10] J. S. Wu and C. T. Chen, A lumped-mass TMM for free vibration analysis of a multi-step Timoshenko beam carrying eccentric lumped masses with rotary inertias, *Journal of Sound and Vibration,* 301 (2006) 878-897.

[11] J. S. Wu and C. T. Chen, A continuous-mass TMM for free vibration analysis of non-uniform beam with various boundary conditions and carrying multiple concentrated elements, *Journal of Sound and Vibration,* 311 (2008) 1420-1430.

[12] Z. Y. Ai and Q. S. Wang, Transfer matrix solutions to axisymmetric and non-axisymmetric consolidation of multilayered soils, *Acta Mechanica*, 211 (2010)155-172.

[13] A. Liew and N. S. Feng, On using the transfer matrix formulation for transient analysis of nonlinear rotor-bearing systems, *International Journal of Rotating Machinery,* 10 (6) (2004) 425-431.

[14] X. T. Rui and B He, Discrete time transfer matrix method for multibody system dynamics, *Multibody System Dynamics,* 14 (2005) 317-344.

[15] S. C. Hsieh and J. H. Chen, A modified transfer matrix method for the coupled lateral and torsional vibrations of symmetric rotor-bearing systems, *Journal of Sound and Vibration*, 289 (3) (2006) 294-333.

[16] S. C. Hsieh and J. H. Chen, A modified transfer matrix method for the coupling lateral and torsional vibrations of asymmetric rotor-bearing systems, *Journal of Sound and Vibration,* 312 (4-5) (2008) 563-571.

[17] H. H. Hertz, *Hertz's miscellaneous papers*, MacMillan, London, EN (1896).

[18] H. Wu and J. W. Wang, Study on the calculating method of radial stiffness of tapered roller bearing, *Lubrication Engineering*, 33 (2008) 39-43.

[19] H. Wu and J. W. Wang, Calculating Method for damping of Tapered Roller Bearings, *Bearing* (2) (2009) 5-9.

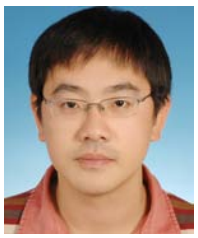

Hao Wu received his Ph.D degree in Mechanical Design and Theory from East China University of Science and Technology, Shanghai, China. His current research interests include inspection of special equipments and vibration of elevators.

Qi An is a professer in the Department of Mechanical and Power Engineering, East China University of Science and Technology, Shanghai, China. His current research interests include tribology and dynamics of bearing-rotor system.